Ab initio electronic structure calculations for point defects in CoAl and CoGa

N. Stefanou, R. Zeller, and P. H. Dederichs
Institut für Festkörperforschung, Kernforschungsanlage Jülich, Postfach 1913, D-5170 Jülich, Federal Republic of Germany
(Received 22 July 1986)

Self-consistent, first-principles calculations are presented for the electronic structure of some point defects in the binary alloys CoAl and CoGa. All possible structural defects—i.e., antistructure atoms and vacancies—as well as $3d$ transition-metal impurities on both sublattices are considered. The calculations are based on the Korringa-Kohn-Rostoker Green's-function method and on density-functional theory in the local-spin-density approximation. The calculated densities of states, charge transfers, and magnetic moments are discussed and compared with the results of other theoretical calculations and the available experimental data.

I. INTRODUCTION

The electronic and magnetic properties of CoM (M = Al,Ga) intermetallic compounds have been the focus of interest of many experimental investigations in recent years. The CoAl and CoGa systems are isoelectronic and exhibit similar behavior. The β phase in these binary alloys crystallizes in the $B2$ (CsCl) structure and persists over a wide composition range: 46–58 at. % Co for CoAl (Ref. 1) and 44–65 at. % Co for CoGa (Ref. 2). The perfectly ordered compounds are nonmagnetic,[3,4] but even small disorder leads to the occurrence of local moments.[1–14] For deviations from stoichiometry, two kinds of structural defects are mainly responsible: vacancies on the Co sublattice and Co antistructure (AS) atoms on the M sublattice, these two types of defects being present even at the equiatomic composition.[5–8] There is a common agreement in the literature that Co AS atoms are responsible for the magnetic properties of these compounds and several authors have tried to deduce from magnetic measurements the moment per Co AS atom. It is widely believed that each Co AS defect is associated with an effective moment of $\sim 5\mu_B$,[3,5,6,7,9] but also more complex models have been proposed ascribing magnetic behavior only to clusters of AS atoms while a single AS defect carries no moment.[4,10] Moreover, above a critical Co concentration of 60.6 at. % for CoAl, magnetic interactions between local moments lead to the appearance of a permanent magnetization at low temperatures.[3] In CoGa Meisel *et al.*[9,11] identified also at low temperatures a phase transition from a spin glass to a ferromagnetic regime, at a concentration of 56 at. % Co, and proposed a magnetic phase diagram for slowly cooled CoGa alloys in the β phase. It must be pointed out that the distribution of the structural defects is very sensitive to the heat treatment which is used. Alloys quenched from high temperatures contain heavy concentrations of Co vacancies as well as large clusters of magnetic defects, as is apparent from neutron scattering experiments.[2] On the other hand, in slowly cooled samples there are many fewer vacancies and the Co AS atoms are more homogeneously distributed than in quenched alloys.[2,4]

The study of further alloy series of the type $Co_2Ga_{2-x}T_x$ ($0<x<1$), where T is a $3d$ transition metal has also attracted special interest. Magnetization, neutron and x-ray diffraction as well as small-angle neutron scattering experiments, together with Mössbauer studies have been performed in order to investigate the structural and magnetic properties of these compounds.[15–22] It was found that Ti, V, Cr, Mn, and Fe exercise site selectivity by substituting for Ga atoms. As $x=1$ is approached in the alloy series, the transition-metal atoms exhibit a preference for one of two apparently identical Ga sites, resulting in the doubly ordered Heusler structure.[15,16] For Ni, neutron diffraction data are consistent with a model in which Ni atoms favor Co sites with displaced Co atoms moving to the Ga sublattice. On the other hand, for Cu the experimental results do not allow one to discriminate at small dilutions between the situations where Cu atoms occupy Ga sites or are equally distributed on all sites.[20] Diffuse neutron scattering data in $Co_2Ga_{2-x}T_x$ (T = Ti,V,Cr,Mn,Fe) suggest that Cr, Mn and, Fe atoms are magnetic and behave analogously to the Co AS defects, whereas Ti and V atoms do not carry a moment. Ferromagnetism is observed as the transition-metal concentration increases above a critical value corresponding to $x\simeq 0.50$, 0.25, and 0.10 for Ti, V, and Cr alloys, respectively.[15,16] In the case of Mn and Fe the critical concentration was reported to be above 1.25 at. % Mn or Fe substitutions.[17] For T = Ni,Cu the transition to the ferromagnetic regime was observed at $x\simeq 0.45$ and 0.40, respectively.[20]

From theoretical point of view, the band structure of the ordered stoichiometric CoAl and CoGa compounds has been investigated by several authors,[23–26] but there are very few calculations of the electronic structure of point defects in these alloys. Benesh and Ellis[27] performed self-consistent cluster calculations in order to describe the electronic structure of isolated transition-metal impurities T (= Ti,V,Cr,Co) in CoGa, using a variational linear combination of atomic orbitals (LCAO's) scheme. In general, they find a strong dependence on the size of the cluster. The largest considered clusters $TCo_8Ga_6Ga_{12}$ turned out to be nonmagnetic. Recently, Koch *et al.*[28,29] performed first-principles Green's-function calculations for vacancies in VAl, FeAl, CoAl, NiAl, and CoGa by the linear muffin-tin orbital (LMTO) method in the atomic-sphere approximation (ASA). In

these calculations it is explicitly assumed that only the impurity potential is perturbed.

Since the cluster calculations are not conclusive with respect to the magnetic properties of these complicated systems, a more sophisticated numerical treatment is desirable. This is the reason we have started the present calculation, which is, in principle, similar to the one of Koch *et al.*,[26,28,29] but in addition includes also the perturbation of the neighboring atoms. In a previous paper we have reported results for the electronic structure of AS Co atoms and Co vacancies in CoAl.[30] The aim of the present work is to obtain a more complete picture of the behavior of intrinsic defects and $3d$ impurities in CoAl and CoGa. In addition to the Co AS atoms we calculate the electronic structure of M AS atoms as well as Co and M vacancies. We consider also all $3d$ impurities on both sublattices and investigate the magnetic behavior of the different defects in the CoM systems.

This paper is organized as follows: Sec. II is devoted to the description of our calculational method. In Sec. III we discuss our results and in Sec. IV we compare them to the available experimental data.

II. CALCULATIONAL METHOD

Our calculational method is based on the multiple scattering theory. The Green's function of the electrons, which are multiply scattered by a collection of nonoverlapping muffin-tin potentials centered at positions $\mathbf{R}^n$ is expanded into eigensolutions of these spherically symmetric local potentials:[31,32]

$$G(\mathbf{r}+\mathbf{R}^n,\mathbf{r}'+\mathbf{R}^{n'};E)=-i\delta_{nn'}\sqrt{E}\sum_{L}Y_L(\hat{\mathbf{r}})R_l^n(r_<,E)H_l^n(r_>,E)Y_L(\hat{\mathbf{r}}')+\sum_{L,L'}Y_L(\hat{\mathbf{r}})R_l^n(r,E)G_{LL'}^{nn'}(E)R_{l'}^{n'}(r',E)Y_{L'}(\hat{\mathbf{r}}')\ , \quad (1)$$

in Rydberg atomic units. The position vectors $\mathbf{r},\mathbf{r}'$ are restricted to the Wigner-Seitz cell and $r_<,r_>$ are the smaller and larger of $r=|\mathbf{r}|$ and $r'=|\mathbf{r}|$. The subscript $L=(l,m)$ denotes angular momentum quantum numbers and Y_L are real spherical harmonics. The irregular H_l^n and regular R_l^n solutions of the radial Schrödinger equation for the nth muffin-tin potential at energy E are defined by their asymptotic behavior outside the muffin-tin sphere of radius R_{MT} ($r>R_{MT}$):

$$\begin{aligned}H_l^n(r,E)&=h_l(r\sqrt{E})\ ,\\ R_l^n(r,E)&=j_l(r\sqrt{E})-i\sqrt{E}\,t_l^n(E)h_l(r\sqrt{E})\ ,\end{aligned} \quad (2)$$

where j_l,h_l are the spherical Bessel and Hankel functions and t_l^n the usual t matrix for the nth single potential.

The information about the multiple scattering between muffin-tins is contained in the structural Green's function matrix $G_{LL'}^{nn'}$. It can be related to its counterpart for the host crystal by an algebraic Dyson equation:

$$G_{LL'}^{nn'}(E)=G_{LL'}^{onn'}(E)+\sum_{n'',L''}G_{LL''}^{onn''}(E)\{t_{l''}^{n''}(E)-t_{l''}^{on''}(E)\}G_{L''L'}^{n''n'}(E)\ , \quad (3)$$

where the o superscript refers to the host. This equation describes correctly and in a very efficient way the embedding of the defect into the ideal crystal. In our calculation the angular momentum expansion in the Green's functions includes s, p, and d electrons, and the perturbation induced by the defect is considered to be extended up to the first shell of neighboring atoms. The perturbation of outer host shells is neglected. The resulting 81×81 matrix equation (3) is solved using group theoretical methods, which reduce the computational effort.[32] The one-electron effective potentials of the nine-atom cluster, consisting of the defect and its eight first-nearest neighbors, are determined self-consistently in the framework of density functional theory. Exchange and correlation effects are included through the local spin-density approximation of von Barth and Hedin with the constants as given by Moruzzi *et al.*[33] The necessary charge density is obtained for the valence states by complex energy integration of the Green's function up to the host Fermi level E_F using 32 complex energies[34] and by considering the core states as frozen. The use of an improved iteration scheme[35] accelerates considerably the convergence of the self-consistency iterations.

The host crystal potential was calculated self-consistently by the augmented spherical wave (ASW) band-structure method[36] with a lattice constant of 5.409 (5.442) a.u. for CoAl (CoGa). Since for the construction of the host Green's-functions bands in a broad energy range are needed, including the Ga $3d$ states and up to 20 (18) eV above E_F for CoAl (CoGa), this potential is used in an augmented-plane-wave (APW) band structure program in order to obtain the expansion coefficients of the Bloch function. Using these coefficients we calculate the host structural Green's functions by a Brillouin-zone integral and a Kramers-Kronig transformation.[31,32] The necessary Brillouin-zone integrations are performed by the tetrahedron method with 321 points in the irreducible wedge.

Our calculations are limited due to two major approximations. First we completely neglect lattice relaxations around the impurity and their possible effect on the electronic structure. Secondly the host potential perturbations are restricted to the first shell. Therefore we cannot say anything about induced charge perturbations and moments of more distant atoms, e.g., the next-nearest-neighbor atoms. From our experience with calculations for impurities in Pd (Ref. 37) where potential perturbations in up to three shells are taken into account, we know that the inclusion of more distant shells has very little effect on the local behavior. Therefore, we expect that the

present results for the impurity and the nearest neighbors change only very little if longer-ranged perturbations are included.

III. RESULTS AND DISCUSSION

A. Band structure of CoAl and CoGa

The band structure of the ordered CoAl and CoGa alloys has been investigated by several authors[23–26] and presents similar features for these two systems. It is characterized by a narrower d band than found in pure Co. The overlap of d-wave functions of the Co atoms is reduced because, being next-nearest neighbors to each other on a simple cubic sublattice with a lattice constant of 5.409 a.u. and 5.442 a.u. for CoAl and CoGa, the distance between Co atoms is larger than in pure Co (4.56 a.u.), leading to the band narrowing. On the other hand, the hybridization with the s and mostly the p levels of M, which lie above the Fermi level, leads to bonding states in the lower part of the d band and to antibonding states in the region above E_F. Since the bonding states are mostly centered at the Co site the number of Co d electrons considerably increases and the number of M s and p electrons decreases compared to the situations in elemental Co and M, respectively. A total charge transfer of 0.42 and 0.40 electrons from Al to Co and from Ga to Co is obtained in our band structure calculation, where the charges refer to the number of electrons within Wigner-Seitz spheres of equal size. Our results for the charge transfer agree qualitatively with those of the other theoretical calculations and they are a few hundredths of an electron larger than the LMTO values calculated by Koch and Koenig[26] under similar assumptions. A further consequence of the strong hybridization is that the tendency for magnetism is suppressed. As it is shown in Figs. 1 and 2, the Fermi energy lies in a region of low density of states, between a high peak of mainly $d_{t_{2g}}$ character and a smaller one of

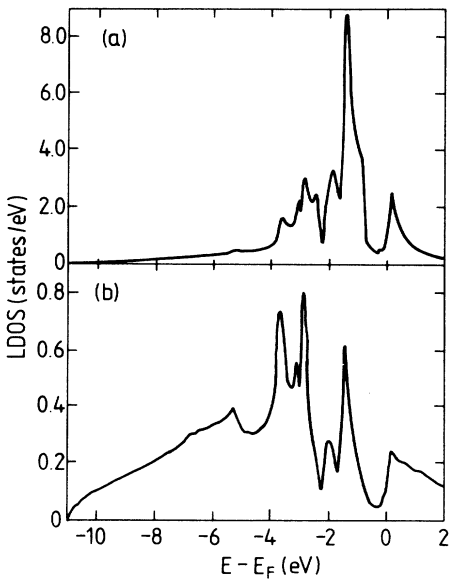

FIG. 1. LDOS of ordered CoAl. (a) Co site, (b) Al site.

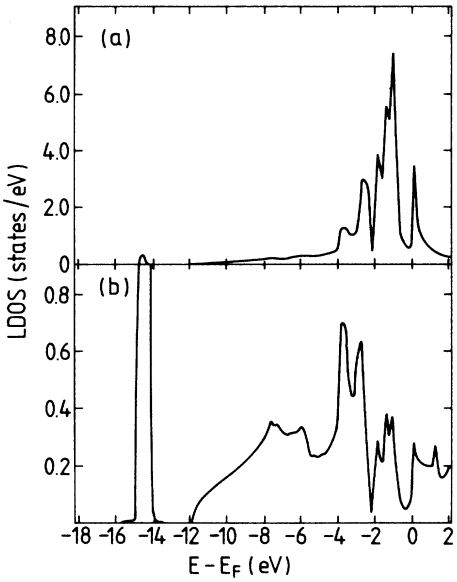

FIG. 2. LDOS of ordered CoGa. (a) Co site, (b) Ga site.

mainly d_{e_g} character, so that the Stoner enhancement is quite small.

An important qualitative difference between these two binary alloys is the presence of the Ga $3d$ states near the bottom of the band. These states are treated as core states in the self-consistent ASW band structure calculation. In the APW calculation the $3d$ states are treated as band states leading to a narrow band at about 14.4 eV below E_F, with a width of about 0.6 eV. In the defect calculations we have included these states in the self-consistency procedure.

B. Electronic structure of vacancies and M AS atoms

As mentioned above, the experimental data show that vacancies occur preferentially on the Co sublattice, but in order to have a more complete picture we calculate here the electronic structure of vacancies on both sublattices. The local densities of states (LDOS's) are shown in Figs. 3 and 4. They are characterized dominantly by s and p states. Electrons tunnel from the neighbors into the vacancy region where a repulsive potential dominates. We calculate 1.20 and 1.06 electrons within the vacancy Wigner-Seitz sphere, on the Co and Al sublattice in CoAl. In the case of CoGa the corresponding values are 1.14 and 0.97 electrons. The calculated vacancy charges are similar to the ones obtained in other systems, e.g., in Cu (Ref. 32) or FeAl (Ref. 29) or Fe and Ni (Ref. 38). On the contrary, Koch and Koenig calculated a much smaller electronic charge for vacancies in CoAl and CoGa: 0.09 and 0.06 electrons on a Co and Al vacancy in CoAl and 0.03 and 0.01 electrons on a Co and a Ga vacancy in CoGa.[26] Their calculation relies on a single site approximation and an adjustment of a constant Madelung potential to satisfy the Friedel's screening rule. Due to the low density of states at the Fermi level for these binary alloys the total screening charge is quite insensitive to the strength of the defect potential, so that this procedure leads to very repul-

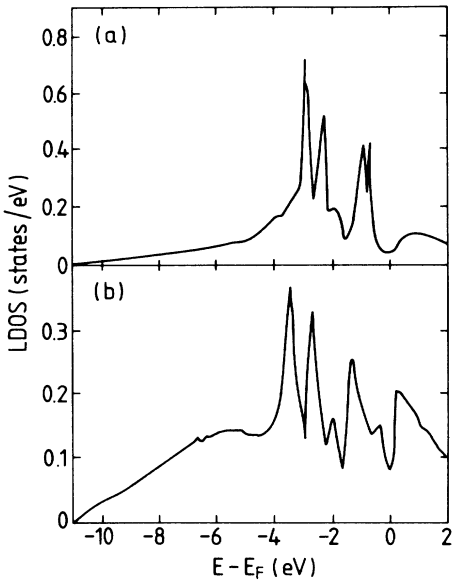

FIG. 3. LDOS of vacancy in CoAl on the Al sublattice (a) and on the Co sublattice (b).

sive vacancy potentials, which strongly repel the electrons out of the vacancy cell. In the present calculation the modification of potentials on the sites neighboring the vacancy are also taken into account in a self-consistent way and consequently the calculated charge transfer into the vacancy should be much more reliable.

The LDOS's on the Al and Ga AS atoms are shown in Figs. 5 and 6. In both cases, the AS M s and p states are shifted to lower energies compared to the M states in ordered CoM, so that a sharp s peak near the bottom of the band occurs. The number of electrons on the AS Al is increased by 0.38 and on the AS Ga by 0.56 with respect to

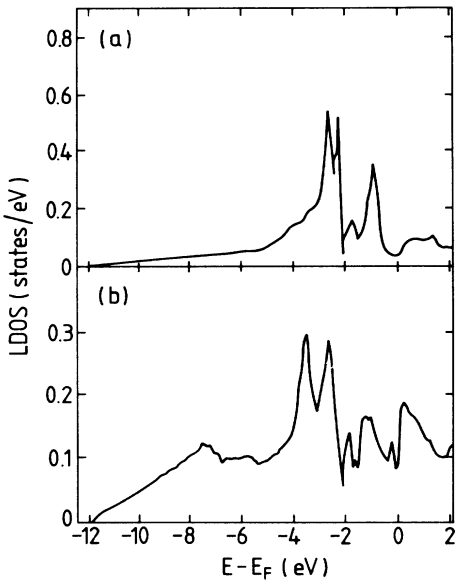

FIG. 4. LDOS of vacancy in CoGa on the Ga sublattice (a) and on the Co sublattice (b).

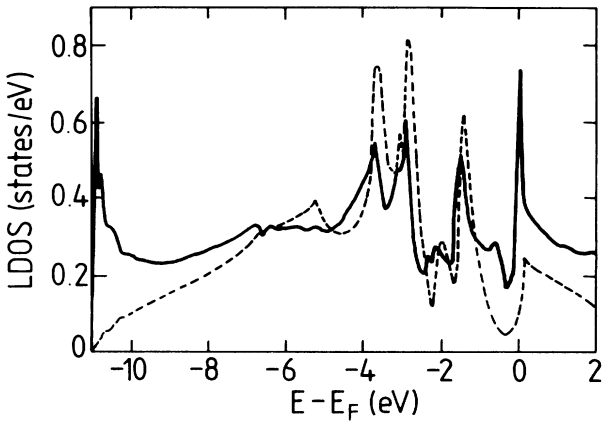

FIG. 5. LDOS of AS Al atom (solid line) and Al atom of ordered CoAl (dashed line).

the corresponding M electronic charge in the pure host. This can be explained by the fact that the AS Al and Ga atoms have no nearest-neighbor Co atoms which would push up their s and p states and which would lead to an appreciable charge transfer. Therefore the AS Al and Ga atoms are practically neutral. If we define the cluster neutrality as the charge transfer difference between the defect and the host system summed over all nine perturbed atoms, we find an almost neutral cluster in all the cases (Table I).

C. 3d impurities on the M sublattice

We now discuss the electronic structure of the 3d-transition impurities on the M sublattice in the CoM systems, including the case of Co AS atoms. The electronic structure of these defects is strongly influenced by the large overlap of the impurity d electrons with d electrons of the eight nearest-neighbor Co atoms. We illustrate the situation explicitly in the case of AS Co. The d overlap is much larger than the one between next-nearest Co neighbors in the ordered alloys. The results of paramagnetic calculations, not allowing for spin polarization, are shown in Figs. 7(a) and 8(a). Due to the strong hybridization, the LDOS is split into a bonding state at lower energies and an antibonding state at higher energies. Both regions are separated by a deep minimum. The resulting LDOS is

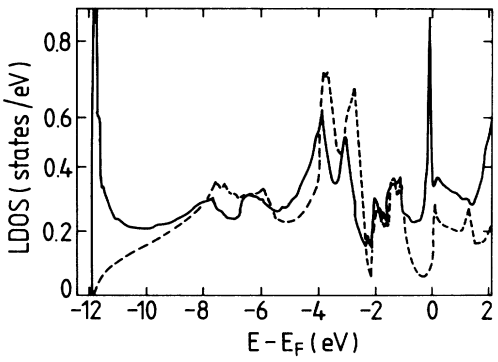

FIG. 6. LDOS of AS Ga atom (solid line) and Ga atom of ordered CoGa (dashed line).

TABLE I. Point defects in CoAl and CoGa. Number of electrons in the impurity N_{imp}, cluster neutrality Δq_{cl}, moment in the impurity M_{imp} and in the nine-atom cluster M_{cl}.

CoAl Al sublattice	Vacancy	^{22}Ti	^{23}V	^{24}Cr	^{25}Mn	^{26}Fe	^{27}Co	^{28}Ni	^{29}Cu	^{13}Al
N_{imp}	1.06	21.34	22.50	23.71	24.78	25.87	27.08	28.17	29.16	12.58
Δq_{cl}	−0.00	−0.01	−0.02	−0.01	−0.01	−0.01	−0.00	0.00	0.00	0
M_{imp} (μ_B per atom)	0	0	0	2.47	3.32	3.00	1.22	0	0	0
M_{cl} (μ_B)	0	0	0	3.02	4.54	4.81	2.06	0	0	0
CoAl Co sublattice	**Vacancy**	**^{22}Ti**	**^{23}V**	**^{24}Cr**	**^{25}Mn**	**^{26}Fe**	**^{27}Co**	**^{28}Ni**	**^{29}Cu**	**^{13}Al**
N_{imp}	1.20	21.68	22.87	24.05	25.21	26.33	27.42	28.45	29.41	12.96
Δq_{cl}	0.01	0.01	0.01	0.01	0.01	0.01	0	−0.00	0.00	0.01
M_{imp} (μ_B per atom)	0	0	1.78	1.79	0	0	0	0	0	0
M_{cl} (μ_B)	0	0	1.99	1.84	0	0	0	0	0	0
CoGa Ga sublattice	**Vacancy**	**^{22}Ti**	**^{23}V**	**^{24}Cr**	**^{25}Mn**	**^{26}Fe**	**^{27}Co**	**^{28}Ni**	**^{29}Cu**	**^{31}Ga**
N_{imp}	0.97	21.17	22.35	23.58	24.68	25.76	26.92	28.08	29.10	30.60
Δq_{cl}	−0.01	−0.01	−0.02	−0.01	−0.01	−0.01	−0.01	−0.00	0.00	0
M_{imp} (μ_B per atom)	0	0	0	2.02	3.36	3.28	2.09	0	0	0
M_{cl} (μ_B)	0	0	0	2.69	4.50	5.16	3.49	0	0	0
CoGa Co sublattice	**Vacancy**	**^{22}Ti**	**^{23}V**	**^{24}Cr**	**^{25}Mn**	**^{26}Fe**	**^{27}Co**	**^{28}Ni**	**^{29}Cu**	**^{31}Ga**
N_{imp}	1.14	21.69	22.87	24.06	25.19	26.31	27.40	28.44	29.39	31.15
Δq_{cl}	0.01	0.01	0.01	0.01	0.01	0.00	0	0.00	0.00	0.01
M_{imp} (μ_B per atom)	0	0	1.04	0.83	0	0	0	0	0	0
M_{cl} (μ_B)	0	0	1.11	0.83	0	0	0	0	0	0

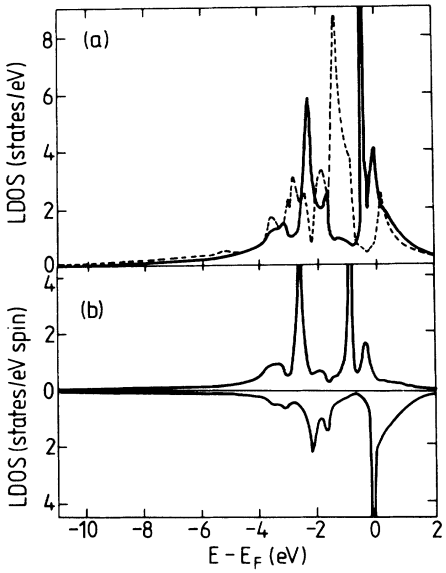

FIG. 7. (a) LDOS of paramagnetic AS Co atom (solid line) and Co atom of ordered CoAl. (b) LDOS of spin polarized AS Co atom (upper curve: majority spin states; lower curve: minority spin states).

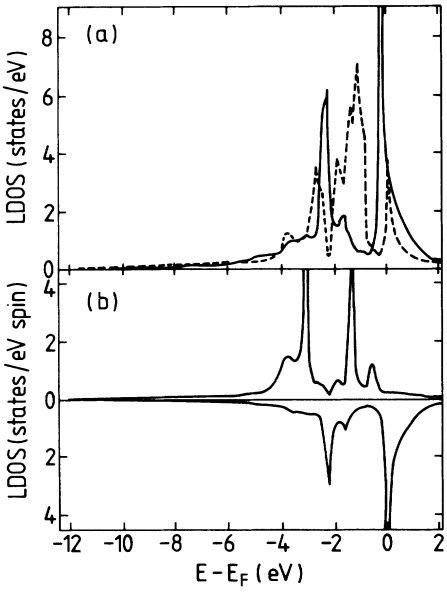

FIG. 8. (a) LDOS of paramagnetic AS Co atom (solid line) and Co atom of ordered CoGa. (b) LDOS of spin-polarized AS Co atom (upper curve: majority spin states; lower curve: minority spin states).

similar to the DOS of bcc transition metals, reflecting the local symmetry of the AS atom and its eight Co neighbors. Since the antibonding peak is close to the Fermi energy, the LDOS at E_F is quite high indicating an instability which leads to the formation of a local moment. The total number of electrons on the AS atom is appreciably smaller than the one on the host Co atoms (Table I). This is due to the broadening of the local d bands induced by hybridization which pushes d states above the Fermi level. Partly this is also a consequence of the missing M nearest neighbors, so that the sp-d hybridization leading to bonding hybrids at lower energies is not so effective as for the host Co atoms. As a result there is no appreciable charge transfer to the AS Co atoms. We obtain a charge of 27.08 electrons for the Co AS atom in CoAl and a slightly smaller charge of 26.92 for the Co AS atom in CoGa.

Spin-polarized calculations yield the spin-split densities of states shown in Fig. 7(b) for CoAl and Fig. 8(b) for CoGa. For the Co AS atom in CoAl we obtain a moment of $1.22\mu_B$, smaller than in elemental Co. The neighboring Co atoms are weakly polarized with a moment of $0.10\mu_B$ per atom, so that the total moment of the cluster of nine Co atoms is $2.06\mu_B$. For CoGa the AS Co atom has a larger moment, $2.09\mu_B$. Also the nearest neighbors carry a slightly larger moment of $0.17\mu_B$ per atom. Consequently a total magnetic moment of $3.49\mu_B$ is ascribed to the nine atom cluster. The results of paramagnetic calculations for $3d$ impurities on the Al site in CoAl are shown in Fig. 9. The corresponding results for CoGa are very similar and therefore not given here. For the Ti impurity we obtain a broad antibonding d peak above the Fermi energy and a weaker bonding feature at about 2 eV below E_F. With increasing valence the antibonding peak shifts to lower energies and more intensity is transferred to the bonding peak. For Cr, Mn, and Fe the antibonding peak is located close to the Fermi energy, so that the LDOS at E_F is quite high. Spin-polarized calculations therefore yield Cr, Mn, and Fe to be magnetic with moments of 2.47 (2.02) μ_B for Cr in CoAl (CoGa), 3.32 (3.36) μ_B for Mn and 3.00 (3.28) μ_B for Fe (see Table I). The corresponding spin-split LDOS are shown in Fig. 10 for Cr, Mn, Fe, and Co in CoAl. Again the LDOS of these impurities in CoGa are very similar and not given here. For V and Ni impurities the antibonding peak is still close to the Fermi energy. However, the LDOS at E_F is rather small so that these impurities are nonmagnetic, both in CoAl and CoGa, as is confirmed by spin-polarized calculations.

The disagreement between our results and those of Benesh and Ellis,[27] who found Cr and Co impurities on the Ga sublattice in CoGa nonmagnetic is most likely due to the fact that their 27-atom cluster is inadequate to obtain converged results for the magnetic properties of these alloys. This is quite plausible since, as we have shown, the occurrence of a local moment in CoGa depends strongly on the LDOS at E_F of these impurities which cannot be calculated reliably in a cluster calculation. Moreover, the clusters in general are not stoichiometric and the outer shell contains either Co or Ga atoms. Both might complicate the convergence behavior as a function of the cluster size.

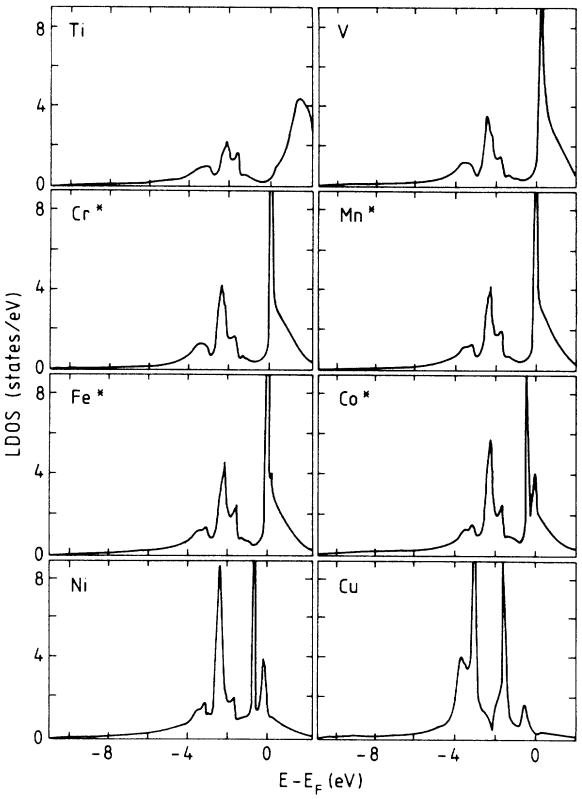

FIG. 9. Paramagnetic LDOS of $3d$ impurities in CoAl on the Al sublattice (* denotes non-spin-polarized calculation).

D. $3d$-impurities on the Co sublattice

The behavior of $3d$ impurities on the Co sublattice is quite different from the previous case. The d-d interaction and the resulting splitting of the d band is rather weak, since the Co atoms are now next-nearest neighbors to the impurity. Similar to pure CoM there is however a strong d-s and d-p hybridization with the neighboring Al or Ga atoms. The calculated paramagnetic LDOS of the impurities in CoAl are shown in Fig. 11. In all cases we observe a single sharp d state and some additional broader d intensity within the range of the CoM d band. Whereas for the Ti impurity the narrow d-peak is still located slightly above E_F, for V and Cr the peak is centered quite close to E_F. Therefore, one expects the formation of local moments for V and Cr. The results of spin-polarized calculations are shown in Fig. 12. The calculated local moments are 1.78 (1.04) μ_B for V and 1.79 (0.83) μ_B for Cr in CoAl (CoGa). The eight M neighbors are weakly polarized so that the resulting cluster moment is slightly higher. For Mn and Fe impurities the situation is different. The local d peak is shifted below the Fermi energy and the LDOS at E_F is very low. Indeed, spin-polarized calculations show that Mn and Fe are not magnetic. This is quite surprising since it is usually Mn which has the biggest moment of all $3d$ impurities in a given host, e.g., in Cu or Ag.[31,32] The physical reason for this unusual behavior is the strong d-sp hybridization with the host M

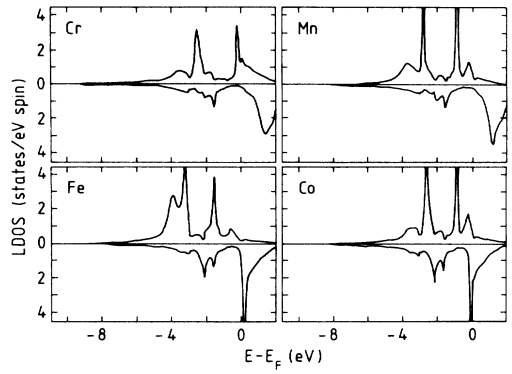

FIG. 10. LDOS of magnetic $3d$ impurities in CoAl on the Al sublattice (upper curves: majority spin states; lower curves: minority spin states).

atoms which pushes the $3d$ levels of these impurities down to lower energies and kills the local moment. In this respect the behavior is quite similar to the case of the pure CoM alloy. Therefore we also observe a rather large charge transfer to the $3d$ impurity, ranging from 0.21 (0.19) for Mn in CoAl (CoGa) to 0.45 (0.44) for Ni. On the contrary, for the early transition-metal impurities (Ti,V) the charge transfer reverses, due to the increase of the atomic $3d$ level. We have investigated the transition from a magnetic solution for Cr in CoAl to a nonmagnetic solution for Mn in more detail by performing calculations for fictitious noninteger nuclear charges between $Z=24$ (Cr) and $Z=25$ (Mn). In Fig. 13 we have plotted

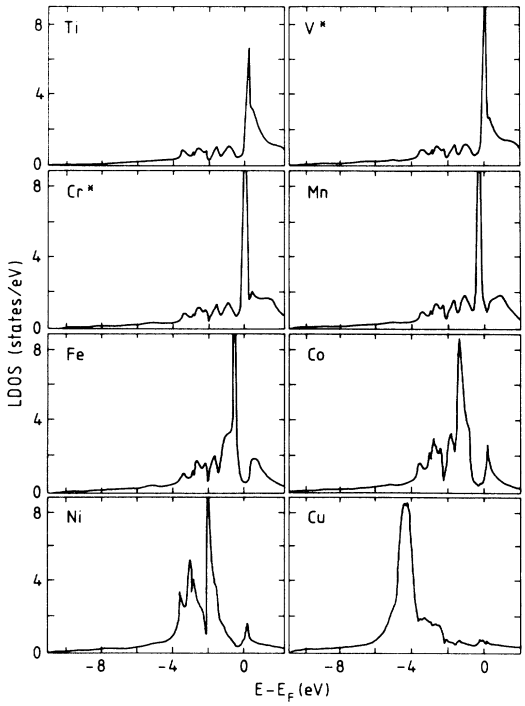

FIG. 11. Paramagnetic LDOS of $3d$ impurities in CoAl on the Co sublattice (* denotes non-spin-polarized calculation).

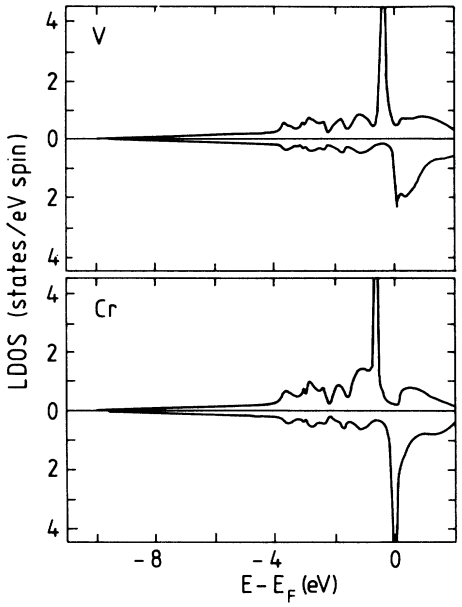

FIG. 12. LDOS of magnetic $3d$ impurities in CoAl on the Co sublattice (upper curves: majority spin states; lower curves: minority spin states).

the resulting local moment versus the impurity nuclear charge. The moment vanishes for $Z>Z_c=24.46$. In the vicinity of this transition the magnetic moment is proportional to $(Z_c-Z)^{1/2}$, as expected for a second-order phase transition.

IV. COMPARISON WITH EXPERIMENTS

In the case of Co AS atoms in CoAl our calculation confirms the experimental result that Co AS atoms are magnetic. It also verifies the speculation proposed in most of the experimental publications on this subject, that localized moments due to a single Co AS atom are ascribed to a magnetic cluster associated with a group of nine Co atoms.

Quantitative comparison of our value for the local magnetic moment with the experimental data is rather difficult because of disorder, clustering of Co AS atoms and

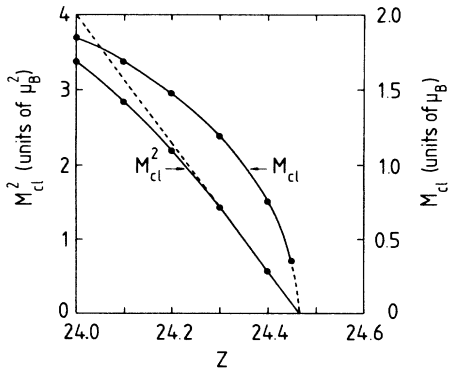

FIG. 13. Magnetic transition in the $3d$-series impurities on the Co sublattice in CoAl (see the text).

magnetic interaction between them, not taken into account in our calculation but occurring in the real alloy. On the other hand, the interpretation of the experimental data is also a difficult problem related to the questions how to correlate magnetic susceptibility or magnetization measurements with the isolated local moments and what is the correct number of AS atoms for a given Co concentration. Extrapolating their 4.2 K data for the magnetization to zero external field Butler and co-workers[1] found saturation moments between $1.5\mu_B$ and $2.5\mu_B$ per excess Co atom for the data between 51% and 58% Co which rather agree with our value. Sellmyer *et al.*[3] derived local effective moments of $5.9\mu_B$ per AS Co from the temperature dependence of the susceptibility at concentrations 50.4% and 50.6% Co. The concentration of Co AS atoms was defined using a simple excess model which means that the presence of vacancies was completely neglected. In this way, underestimating the number of Co AS atoms the moment is overestimated. Wachtel and coworkers[5,7] used a defect mechanism taking into account vacancies on Co sublattice and Co AS atoms. They deduce the AS Co concentration from the Co vacancy concentration which they determine from a Simmons-Baluffi experiment. Thus, correlating the measured Curie constant with the local effective moment they found values depending on the concentration and varying between $0.63\mu_B$ and $5.32\mu_B$ per AS Co in the composition range from 49.8—53.5% Co (Ref. 5) and between $2.4\mu_B$ and $5.3\mu_B$ per AS Co for concentrations from 49% to 55% Co (Ref. 7), but remaining quite stable ($\sim 5\mu_B$) on the Co-rich side compositions. The value of $\mu_{\text{eff}} \simeq 5\mu_B$ corresponds to a spin $S \simeq 2$ ($\mu_{\text{eff}} = g[S(S+1)]^{1/2}\mu_B$) and thus a moment of $M \simeq 4\mu_B$ ($M = gS\mu_B$) has to be compared with our results. Finally, Parthasarathi and Beck[12] proposed a formula relating the magnetization to the temperature and the external field. By least-squares fits of the parameters to their experimental data they calculate a moment of $1\mu_B$ on a single Co AS atom for $Co_{0.48}Al_{0.52}$ and $Co_{0.50}Al_{0.50}$.

In the case of CoGa, the same interpretation problems as for CoAl exist in the experimental literature concerning the magnetism of the AS Co atoms. Amamou and Gautier[4] suggested that the localized moments arise from magnetic interaction between AS Co atoms, whereas a single AS Co defect does not carry any moment. Consequently a cluster of AS atoms should be considered. Parthasarathi and Beck[12] ascribed a local moment of about $1\mu_B$ per AS Co atom in $Co_{0.47}Ga_{0.53}$, whereas Cywinski *et al.*[14] analyzing their recent magnetization density data, deduced from neutron diffraction experiments, proposed a moment of $0.49\mu_B$ per AS Co. On the other hand, several authors[5,6,9] deduced from magnetic susceptibility measurements the value of five effective Bohr magnetons per AS Co atom.

Experimental investigations of the structural and magnetic properties of the $3d$-transition series impurities in CoGa have been also performed. As it was pointed out by Booth *et al.*[15–17] Ti, V, Cr, Mn, and Fe impurities occur preferentially on the Ga sublattice. In this context it is interesting that the experimental data show that Cr, Mn, and Fe atoms possess a moment and behave analogously to the Co AS atoms in CoGa, whereas Ti and V impurities do not carry a moment, which is consistent with our results. The magnetic moment on the Cr of $(1.5\pm0.3)\mu_B$ per Cr atom, measured by the small-angle neutron scattering technique in the concentrated $Co_2Ga_{1.2}Cr_{0.8}$ alloy is in satisfactory agreement with the calculated value of $2.02\mu_B$ per Cr atom. Mn and Fe impurities on the Ga sublattice are calculated to have stronger moments than Cr or Co. The calculated moment on the Mn impurity of $3.36\mu_B$ per atom is in good agreement with the experimental value of $(3.01\pm0.16)\mu_B$ per Mn atom measured in the Heusler alloy Co_2MnGa.[39] The same experimental local moment on the Mn is measured in the alloy Co_2MnAl,[39] which is also consistent with our value of $3.32\mu_B$ per atom.

V. SUMMARY AND CONCLUSIONS

We have performed self-consistent *ab initio* calculations in the framework of density functional theory using the local spin-density approximation. The electronic structure of vacancies, AS atoms and $3d$ impurities on both sublattices in the binary alloys CoAl and CoGa is investigated. The embedding of the defect into the ordered compound is described within the Korringa-Kohn-Rostoker (KKR) Green's-function method, considering a cluster of perturbed muffin-tin potentials at the defect and its eight nearest-neighbor sites in an otherwise ideal alloy.

Vacancies on both sublattices contain about one electron within their Wigner-Seitz sphere which is roughly the same value as calculated for vacancies in other systems. $3d$ impurities on both sublattices can be magnetic or not. On the M sublattice Cr, Mn, Co, and Fe are magnetic. The moment is distributed on the impurity and its eight Co neighbors. On the Co sublattice only V and Cr carry a local moment.

Our theoretical results are in agreement with experimental magnetic measurements in $Co_2Ga_{2-x}T_x$ (T=Ti,V,Cr,Mn,Fe) ternary alloys according to which Ti, V, Cr, Mn, and Fe impurities occur preferentially on the Ga sublattice and only Cr, Mn, and Fe carry a moment and behave analogously to the Co AS atoms. In the case of Co AS atom the situation is more delicate. While our values of $2.06\mu_B$ and $3.49\mu_B$ per Co AS atom in CoAl and CoGa, respectively, are still within the scattering of the experimental data they are smaller than the generally accepted value of $4\mu_B$ deduced from susceptibility measurements for the Co-rich CoAl and CoGa alloys. This discrepancy is most likely to be related to experimental difficulties in defining the AS Co concentration, as well as to the effects of vacancies and clustering of Co AS atoms on the local moments. These effects are not taken into account in our calculation but might be of importance in the real alloy.

[1]S. R. Butler, J. E. Hanlon, and R. J. Wasilewski, J. Phys. Chem. Solids **30**, 1929 (1969).
[2]R. Cywinski, J. G. Booth, and R. D. Rainford, J. Phys. F **7**, 2567 (1977).
[3]D. J. Sellmyer, G. R. Caskey, and J. Franz, J. Phys. Chem. Solids **33**, 561 (1972).
[4]A. Amamou and F. Gautier, J. Phys. F **4**, 563 (1974).
[5]E. Wachtel, V. Linse, and V. Gerold, J. Phys. Chem. Solids **34**, 1461 (1973).
[6]D. Berner, G. Geibel, V. Gerold, and E. Wachtel, J. Phys. Chem. Solids **36**, 221 (1975).
[7]R. Meyer, E. Wachtel, and V. Gerold, Z. Metallkd. **67**, 97 (1976).
[8]G. L. Whittle, P. E. Clark, and R. Cywinski, J. Magn. Magn. Mater. **28**, 64 (1982).
[9]M. W. Meisel, Wen-Sheng Zhou, J. R. Owers-Bradley, Y. Ochiai, J. O. Brittain, and W. P. Halperin, J. Phys. F **12**, 317 (1982).
[10]D. J. Sellmyer and R. Kaplow, Phys. Lett. **36A**, 349 (1971).
[11]M. W. Meisel, W. P. Halperin, Y. Ochiai, and J. O. Brittain, J. Phys. F **10**, L105 (1980).
[12]A. Parthasarathi and P. A. Beck, Solid State Commun. **18**, 211 (1976).
[13]J. G. Booth and J. D. Marshall, Phys. Lett. **32A**, 149 (1970).
[14]R. Cywinski, D. E. Okpalugo, S. K. Burke, and J. G. Booth, J. Magn. Magn. Mater. **54-57**, 1009 (1986).
[15]J. G. Booth and R. G. Pritchard, J. Phys. F **5**, 347 (1975).
[16]R. Cywinski and J. G. Booth, J. Phys. F **6**, L75 (1976); **7**, 1531 (1977).
[17]R. Cywinski, J. G. Booth, and B. D. Rainford, J. Appl. Cryst. **11**, 641 (1978).
[18]K. Raj, J. I. Budnick, T. J. Burch, R. Cywinski, and J. G. Booth, Physica **86-88B**, 407 (1977).
[19]R. Cywinski, J. G. Booth, and B. D. Rainford, Physica **86-88B**, 404 (1977).
[20]J. G. Booth, R. Cywinski, and J. G. Prince, J. Magn. Magn. Mater. **7**, 127 (1978).
[21]G. L. Whittle and P. E. Clark, Solid State Commun. **33**, 903 (1980).
[22]G. L. Whittle, P. E. Clark, and R. Cywinski, J. Phys. F **10**, 2093 (1980).
[23]V. L. Moruzzi, A. R. Williams, and J. F. Janak, Phys. Rev. B **10**, 4856 (1974).
[24]R. Eibler and A. Neckel, J. Phys. F **10**, 2179 (1980).
[25]K. Pechter, P. Rastl, A. Neckel, R. Eibler, and K. Schwarz, Monatshefte für Chemie **112**, 317 (1981).
[26]J. M. Koch and C. Koenig, Philos. Mag. B **54**, 177 (1986).
[27]G. A. Benesh and D. A. Ellis, Phys. Rev. B **24**, 1603 (1981).
[28]C. Koenig, N. Stefanou, and J. M. Koch, Phys. Rev. B **33**, 5307 (1986).
[29]J. M. Koch, N. Stefanou, and C. Koenig, Phys. Rev. B **33**, 5319 (1986).
[30]N. Stefanou, R. Zeller, and P. H. Dederichs, Solid State Commun. **59**, 429 (1986).
[31]R. Podloucky, R. Zeller, and P. H. Dederichs, Phys. Rev. B **22**, 5777 (1980).
[32]P. J. Braspenning, R. Zeller, A. Lodder, and P. H. Dederichs, Phys. Rev. B **29**, 703 (1984).
[33]V. L. Moruzzi, J. F. Janak, and A. R. Williams, *Calculated Electronic Properties of Metals* (New York, Pergamon, 1978).
[34]R. Zeller, J. Deutz, and P. H. Dederichs, Solid State Commun. **44**, 993 (1982).
[35]H. Akai and P. H. Dederichs, J. Phys. C **18**, 2455 (1985).
[36]A. R. Williams, J. Kübler, and C. D. Gelatt, Jr., Phys. Rev. B **19**, 6094 (1979).
[37]A. Oswald, R. Zeller, and P. H. Dederichs, Phys. Rev. Lett. **56**, 1419 (1986).
[38]H. Akai, R. Zeller, and P. H. Dederichs (unpublished).
[39]P. J. Webster, J. Phys. Chem. Solids **32**, 1221 (1971).